

AN EXTENDED OCTAGONAL RING DYNAMOMETER FOR MEASUREMENT OF FORCES ON A SIMPLE TILLAGE TOOL

A.P. Onwualu

Agricultural Engineering Department
University of Nigeria, Nsukka, Nigeria.

ABSTRACT

The analysis, design, construction, evaluation and use of an extended octagonal ring dynamometer for measurement of draught, vertical force and moment on a simple tillage tool are presented. The dynamometer was used to measure tool forces as functions of depth, rake angle and speed, for a wide plane blade.

The dynamometer was designed for a maximum draught of 4.4 kN, vertical force of 4.0 kN and moment of 2.2 kN-m. Evaluation and calibration showed linear response ($R^2 = 0.99$ to 1.00) for the relationship between applied load and output voltage and no hysteresis effect within the load range was observed. Actual sensitivity obtained were $0.332 \mu \text{ V/N.V}$ for draught, $0.726 \mu \text{ V/N.V}$ for vertical force and $2.5 \mu \text{ V/N-m.V}$ for moment. Maximum cross sensitivity was less than 6%. The dynamometer showed expected response of tool forces as affected by tool depth, rake angle and speed.

KEYWORDS: Tillage, Dynamometer, Extended Octagonal Ring, Force, Soil bin, Draught

1. INTRODUCTION

In soil-tool interaction investigations for tools of complex geometry, it is required to measure three force components along three principal axes and three moments about them. Dynamometers for such systems consist of individual strain gauges and or load cells mounted on relevant locations of a frame that supports the tool, enabling the measurement of individual forces of interest or the six components simultaneously [1, 2, 3, 4]. For symmetrical tools, it is only necessary to measure two force components and a moment. This can be accomplished by mounting strain gauges on the tool bar to form Wheatstone bridges [5]. The problems with such a technique include safety of the gauges, low sensitivity and inaccurate prediction of the performance of the dynamometer. These problems can be eliminated by the use of the Extended Octagonal Ring Dynamometer, EORD [6].

The extended octagonal ring was originally developed for metal cutting machines [7]. It has since been adapted and used in farm machinery applications. For tillage applications, it has been used for measuring forces on plane tools in laboratory soil bins [8] and in field applications [9, 10]. With specific mounting arrangements, the dynamometer has been used for non-symmetrical tool studies including the determination of forces acting on a sugar beet topping knife [11]; direct drilling point evaluation [12]; development of rotary tiller blades [13]; and analysis of forces acting on different components of a mouldboard plough [14]. In developing a soil bin test facility, it was required to develop the extended octagonal ring dynamometer as an integral part of the instrumentation and control system. A custom designed and built dynamometer was necessary because of the peculiar nature of the soil bin. This paper presents the analysis, design, construction and

evaluation of the extended octagonal ring dynamometer (EORD).

2. THEORY

The EORD is based on the principles of operation of the simple circular load ring [15, 16, 17, 18, 19]. Figure 1 shows a simple circular load ring for measurement of horizontal (F_x) and vertical force (F_z).

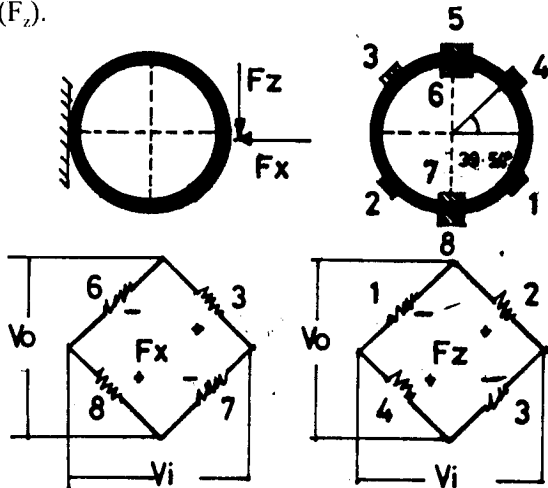


Fig. 1: Simple circular load ring with wheatstone bridge circuits for strain gauges (1-8) V_o = output voltage, V_i = excitation voltage F_x = horizontal force, F_z = vertical force.

The external forces acting on the ring, (F_x and F_z) and the restriction of one end of the ring create a moment which varies with angular position (ϕ) as shown in Fig. 2.

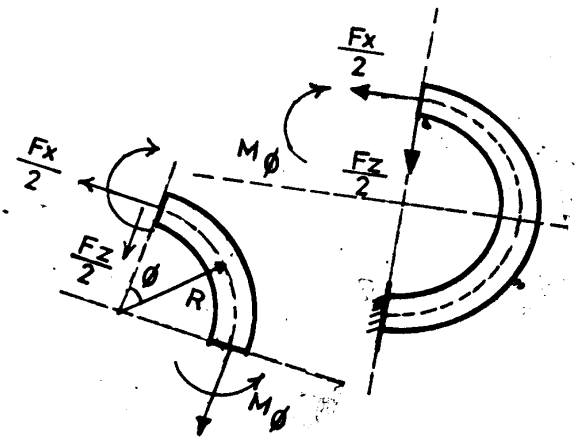


Fig. 2: Forces and moment acting on the load ring F_x = horizontal force, F_z = vertical force, M_ϕ = moment.

The moment (M_ϕ) in the ring of radius R , at any location at an angle ϕ from the point of application of the loads is [6,7]:

$$M_\phi = \frac{F_x R}{2} \left[\frac{2}{\pi} - \sin\phi \right] + \frac{F_z R \cos\phi}{2} \quad (1)$$

for $0 < \phi < \pi$

$$M_\phi = \frac{F_x R}{2} \left[\frac{2}{\pi} - \sin\phi \right] + \frac{F_z R \cos\phi}{2} \quad (2)$$

for $0 < \phi < 2\pi$

Therefore when $\sin \phi = 2/\pi$ (or $-2/\pi$), the bending moment and hence strain in the ring is independent of F_x . The locations on the ring where this condition is met form strain nodes for F_z . This occurs at $\phi = 0.69$ rad (39.54°). Similarly, when $\cos\phi = 0$, the moment and hence the strain is independent of F_z , and this forms the strain node for measurement of F_x ($\phi = \pi/2$ rad or 90°). Strain gauges mounted at these locations can measure these forces simultaneously with little or no cross sensitivity. They are usually connected in two full Wheatstone bridge circuits (Fig.1) for self temperature compensation and high sensitivity.

Using strain energy theory, the strain (ϵ) developed in a thin ring is [7]:

$$\epsilon = \frac{6M_\phi}{Ebt^2} \quad (3)$$

where M_ϕ is the moment, E is the modulus of elasticity, b is the width of the ring and t is the thickness. If the angular positions of the strain nodes ($\phi = 39.54^\circ$ and 90°) are used in equation (1):

$$M_{39.54^\circ} = 0.3856 F_z R \quad (4)$$

$$M_{90^\circ} = -0.1817 F_x R \quad (5)$$

Substituting equations (4) and (5) in equation (3):

$$\epsilon_{39.54^\circ} = \pm \frac{2.31 F_z R}{Ebt^2} \quad (6)$$

$$\epsilon_{90^\circ} = \pm \frac{1.09 F_x R}{Ebt^2} \quad (7)$$

Thus the strains developed in the ring are directly related to the forces, provided the elastic limit of the material is not exceeded and that there is no rotation of the ring. Due to the circular nature of the ring, rigid mountings that ensure this are impossible unless the outside surface of the ring is changed to an octagon as shown in Fig. 3. In so doing, no exact elasticity solution can be obtained.

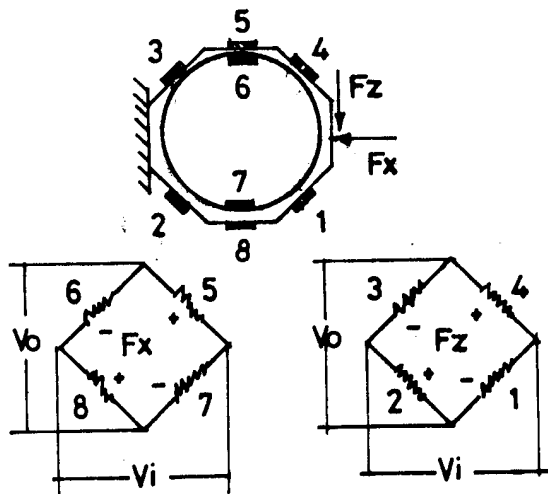


Fig. 3: Simple octagonal ring dynamometer with strain gauge locations (1-8) and bridge circuits V_o = output voltage, V_i = excitation voltage, F_x = horizontal force, F_z = vertical force.

Cook and Rabinowicz [7] found by photoelastic techniques that the strain node for such an octagonal ring occurs at $\phi = 50^\circ$ (instead of 39.54°) for F_z , while that for F_x is unchanged, giving the following equations:

$$\epsilon_{50^\circ} = \pm \frac{1.4 F_x R}{Ebt^2} \quad (8)$$

$$\epsilon_{90^\circ} = \pm \frac{0.7 F_x R}{Ebt^2} \quad (9)$$

The point of application of F_x and F_z , is usually away from the centroid of the dynamometer as Fig. 4, creating a moment which tends to rotate transducer about the z axis.

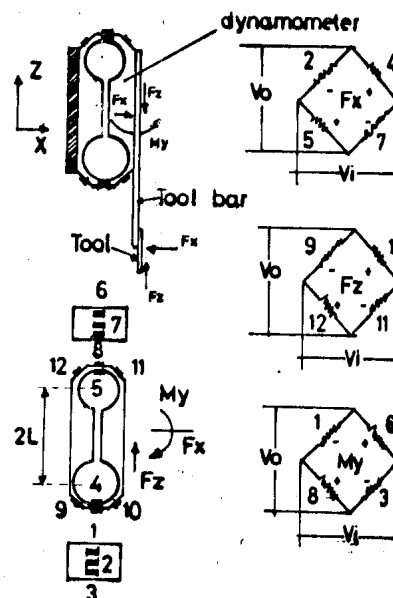


Fig. 4: The extended octagonal ring dynamometer show strain gauge locations (1-2) for horizontal force (F_x), vertical force (F_z) and

moment (My). Vi excitation voltage. Vo = output voltage.

To prevent this, the ring is extended by a thick beam, of length 2L. It is possible to also measure the applied moment by adding two more gauges each at the top and bottom face of the ring shown in Fig. 4. The design of such a ring cot be accomplished by using equations developed for circular extended rings [17, 18]. In addition equations similar to [6] and [7], the strain developed in the ring and the rotation (a) of ring are:

$$\epsilon = \frac{3M}{Ebt^2} \left[\frac{0.36K+0.14}{K^2+1.27K+0.5} \right] \quad (10)$$

$$\alpha = \frac{MR \left[6\pi \left(2K + \frac{\pi}{2} \right) - 24D \right]}{Ebt^2 \left[K^2\pi + 4K + \frac{\pi}{2} \right]} \quad (11)$$

Where:

$$D = 24 \left(2K + \frac{\pi}{2} \right) (2K + \pi K) + C \quad (12)$$

$$C = 3\pi(2 + \pi K)^2$$

$$K = L/R$$

The relationships in (10) and (11) are more useful in graphical form as shown in Fig. 5.

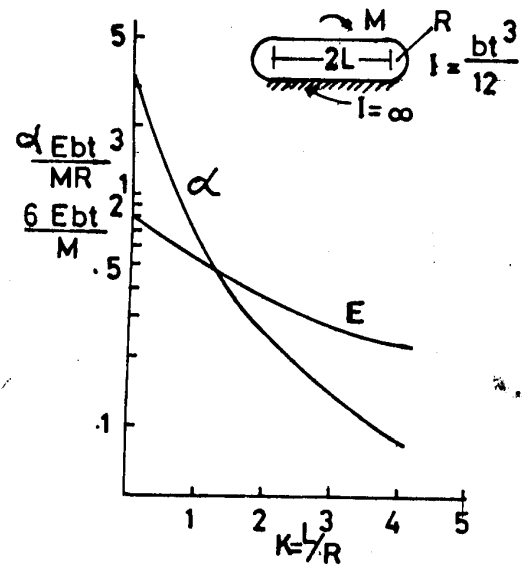


Fig. 5: Moment sensitivity and rigidity relationship for an extended round ring. Source: Ref. (17).

For any value of K, two values K_1 and K_2 can be obtained from the graph such that equations (10) and (11) translate to:

$$\frac{\epsilon Ebt^2}{M} = K_1 \quad (13)$$

$$\frac{\alpha Ebt^2}{MR} = K_2 \quad (14)$$

In equations (12) and (13), K_1 and K_2 are strain and stiffness dimensionless numbers obtained by evaluating the expressions in square brackets in equations (10) and (11) respectively. In the original design [7], there was no provision for measuring F_x , and M_y simultaneously and independently. This can be accomplished by adding four extra strain gauges on the top and bottom faces of the load cell [19,20]. In order to make the transducer output independent of point of application, plates are usually inserted between the load cell and the tool bar and the mounting surface as shown in Fig. 6a. This shifts the strain node for F_z to 34° . The main body of the transducer can be designed in such a way that the plate is part of the body (Fig. 6b).

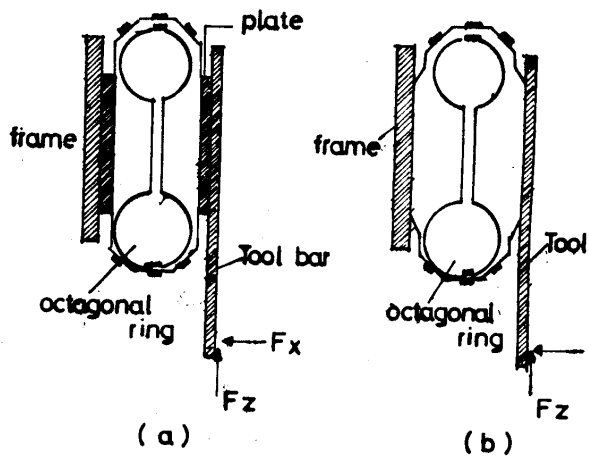


Fig. 6: The use of plates to avoid point locating (a) plate inserted between dynamometer and frame/tool bar (b) plate made an integral part of dynamometer.

In general, once the dynamometer is designed to withstand the applied moment using equations (12) and (13), the strain developed due to the forces and hence the sensitivity can be obtained by generalizing equations (4) and (5) as:

$$\epsilon_{34} = \frac{K_3 F_2 R}{E b t^2} \tag{15}$$

$$\epsilon_{90} = \frac{K_4 F_x R}{E b t^2} \tag{16}$$

The coefficients K_3 and K_4 were obtained empirically as 1.66 and 1.5 respectively by Godwin [6] and 1.9 and 1.6 respectively by O'Doherty [11]. The sensitivity (V_o) of a Wheatstone bridge circuit depends on the applied or excitation voltage (V_e), the gauge factor (F), the strain developed in the material (ϵ) and the number of active arms of the bridge (n) as follows [21]:

$$V_o = \frac{V_i F \epsilon n}{4} \tag{17}$$

3. DESIGN AND DEVELOPMENT OF THE DYNAMOMETER

3.1 Design Considerations

The important criteria and requirements which were considered in designing the extended octagonal ring dynamometer were: load requirement and condition; sensitivity and rigidity; natural frequency of the dynamometer system; cross sensitivity; linearity; stability, space and mounting requirements.

3.2 Design and Description of the Dynamometer

Two extended octagonal ring dynamometers (EORD) were designed and fabricated. One of the rings (EORD1) was designed for low loads (high sensitivity) while the other (EORD2) was designed for relatively large loads (low sensitivity). The design involved an iterative process. Selection of initial trial dimensions was guided by reports in the literature and the design criteria outlined earlier.

Figure 7 shows details of one of the dynamometers (EORD1). The design parameters for the dynamometers are shown in Table 1.

Table 1: design parameters for the dynamometers

Parameter	EORD1	EORD2
F_x , kN	2.2	4.4
F_z , kN	2.0	4.0
M_y , kN, m	1.1	2.2
σ_y , Mpa	525	525
E , GPa	69	69
b , m	0.051	0.051
$2l$, m	0.133	0.178
R , m	0.025	0.029
K	2.66	3.11
K_1	0.3	0.27
K_2	0.18	0.14
K_3	1.66	0.66
K_4	1.5	1.5
Ring thickness (m)	0.005	0.0064
Rotation, deg	0.62	0.64
Max. Strain, F_x (μ strain)	905	1336
Max. Strain, F_z (μ strain)	579	873

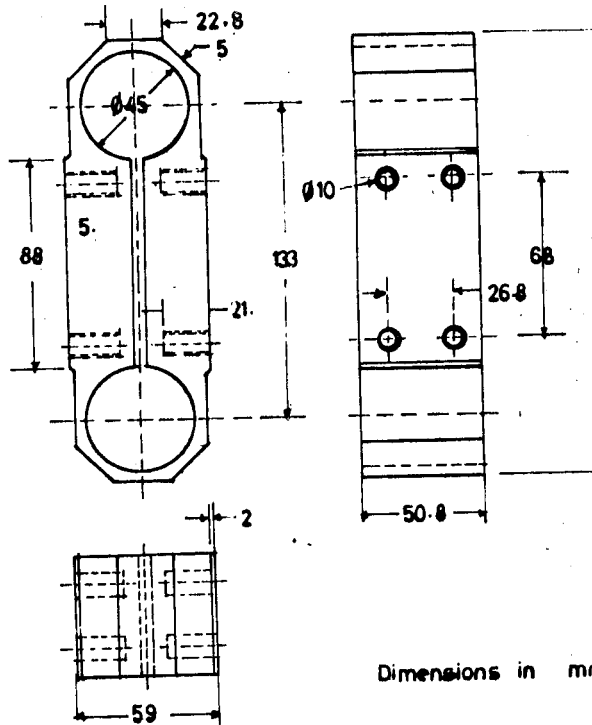


Fig. 7: Details of one of the dynamometers (EORDI).

The estimated maximum loading requirement of the two load cells are shown in Table 1. The loads were estimated based on a maximum tillage tool size of 15 x 15 cm for EORD1 and 30 x 30 cm for EORD2 and noting that the tool would be suspended from a tool bar as shown in Figure 8.

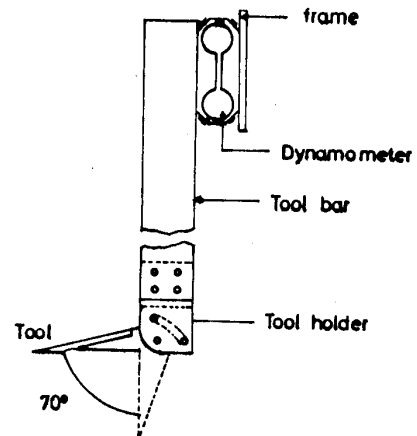


Fig. 8: The dynamometer tool bar, tool holder and tool.

Aluminium alloy, 7075-T6 with a yield stress, σ_y of 525 MPa and Modulus of Elasticity, E of 69 GPa was chosen. To calculate the thickness of the ring, equation (12) was used, noting that:

$$\epsilon = \frac{\sigma_y}{EN} \tag{18}$$

where N is the safety factor based on yield strength ($N = 3$). The parameters used for solving for the thickness (t) in equation (12) and (15) are shown in Table 1, as well as the thickness calculated.

Equation (13) was used to check for the stiffness of the rings under the design loads. Using the parameters in Table 1, the rotation of the top member of the ring about the axis for the two were obtained as presented in the table. These were considered satisfactory. It should be noted however that the actual rotation in practice will be 2 to 3 times the predicted value due to elastic clamping and bending [17].

The maximum strain developed in the ring due to the various loads were estimated by using equations (12), (14) and (15). The values obtained are shown in Table 1. These were considered satisfactory as they were below the recommended maximum strain of 2000 micro-strain [15]. The sensitivity of the bridge circuits were predicted for the different loads using

equation (16) and parameters in Table 1. The actual capacity of the load cells for the forces in X and Z directions, if the loading were through the centroid of the transducer is much higher than the values in Table 1. By using equations (14) and (15) and solving for the forces, the maximum loads were obtained as 5.9 and 5.4 kN for F_x , and F_z , respectively for EORD1, and 12 and 11 kN for F_x and F_z respectively for EORD2.

3.3 Tool Bar Design

The tool bar was designed to withstand the applied loads with minimum deflection. The tool mounting system consists of the dynamometer fixed to the tool mounting plate the tool bar, tool holder and tool arranged as shown in Fig. 8. The system was modelled as a cantilever beam. The maximum load at the free end occurs when the maximum draught acts on the tool which happens for a vertical tool operating at the maximum depth. An allowable maximum deflection of 1 mm was used as the criterion for design.

The deflection (δ_v) at the free end of a cantilever is given in equation (18). The maximum load (P) was taken as the maximum draught the load cell can withstand, the length of the beam (l) is shown in Fig. 8 while the modulus of elasticity (E) of aluminium is in Table 1.

$$\delta_v = \frac{Pl^3}{3EI} \quad (19)$$

The only unknown in equation (18) is the moment of inertia (I) which depends on the cross-section. A hollow rectangular tube was selected in preference to a solid bar because of its better moment of inertia to weight ratio. A cross section of 7.62 x 5.08 x 0.64 cm was found adequate. The natural frequency (ω_o) of the tool mounting system is given as [22]:

$$\omega_o = \sqrt{\frac{k}{m}} = \sqrt{\frac{AE}{mL}} \quad (20)$$

where m is the mass, $k = AE/L$, A is the area of the section and L is the length of the beam. The mass used in equation (19) included that of the dynamometer, tool bar, tool holder and tool. With the relevant dimensions, the natural frequency was obtained as 929 Hz. The maximum frequency reported for forces in tillage is 10 Hz, giving a frequency ratio of 0.01, less than the 0.1 usually recommended [22].

3.4 Computer Based Measurement System

Voltage signals from the dynamometer were acquired by a computer based measurement system which was an integral part of the soil bin measurement and control system [23, 24]. The signals were acquired through an Analog to Digital Converter (ADC), an interface board and a personal computer. The ADC was a 12 bit Successive Approximation Register (SAR) with a resolution of 0.024% of the full scale range. It had a number of special features including software programmable amplifiers and active filters that provided anti-aliasing for the ADC. The measurement was driven by a software developed in QuickBasic which was able to scan the three force channels at a maximum throughput of 2.3 kHz.

The dynamometer system was integrated into a soil bin facility developed at the Department of Agricultural Engineering, Technical University of Nova Scotia, Halifax, Canada. The facility consisted of a stationary bin; common carriage that supported either the tool/penetrometer carriage or the soil processing carriage; an integrated hydraulic power system; instrumentation; computer based data acquisition and control system [23,24,25]. The dynamometer system was attached to

the tool/penetrometer carriage.

4. EXPERIMENTAL METHODS FOR PERFORMANCE EVALUATION

4.1 Dynamometer Calibration Procedure

For calibration, the dynamometers were mounted in the same configuration as they would be used in practice. A static load calibration procedure was used. The three bridges were powered with the same regulated 5 V supply to be used in the experiment and all connections to the measurement system was as planned for the experiment. To measure the voltage output from the bridges, software autozeroing technique was used which involved the measurement system first obtaining the initial unstrained output of the bridges. These were subtracted from subsequent readings by the software to obtain the actual voltage output due to the load increment. For each load increment, the three force channels on the measurement system were scanned 50 times. The average of the 50 samples for each channel was later taken as the voltage output. Simultaneously, a digital voltmeter was used to ensure that the readings were in fact correct. The same procedure was used for unloading.

For the vertical force, the transducer was fixed to the tool mounting plate on the tool carriage in a vertical position as shown in Fig. 9a. A load hanger was used to subject the dynamometer to known weights. The dynamometer was loaded and unloaded in steps and the signal from the three channels monitored as described above.

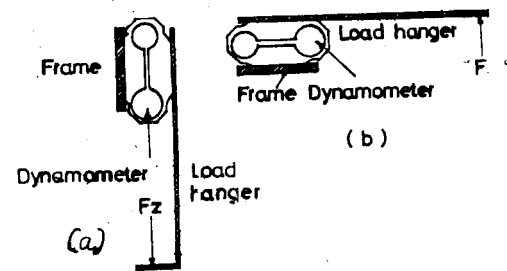


Fig. 9: Loading configuration for calibration (a) vertical force (F_z), (b) horizontal force (F_x).

For the horizontal force and moment, the dynamometer was fixed to a horizontal flat surface and a load hanger with the same moment arm as would be used in the experiment (Fig. 9b). Loading and unloading were in steps and the signals were monitored simultaneously as before.

4.2 Soil Preparation

The bin was filled to a depth of 0.5 m with silty sand (properties shown in Table 2). For all tests, the soil was prepared to an average dry density of 1.5 g/cm², cone index of 0.31 MPa and moisture content (dry basis) of 14%.

Table 2: Soil description

Characteristic	Value
Soil type	Silty sand
Clay content (<0.002 mm)	2.5%
Silt content (0.002-0.05mm)	5.0%
Sand content (>0.05mm)	92.5%
Cohesion	0 kPa
Angle of internal friction	30°
Adhesion	7.66 kPa
Angle of soil-metal friction	15.22°
Opt. moisture content (dry basis)	12.2%
Maximum dry density	1.73g/cm ³

The soil was prepared to the desired density and moisture content by using the soil processing carriage which was equipped with a powered rotary tiller, roller, levelling blade and a boom sprayer. The levelling blade was used to level the surface of the soil. The roller was subsequently used, allowing it to compact the soil using only its weight and matching the speed of rotation with that of the carriage to avoid slippage. At the end

of each soil preparation, a hydraulically powered, computer controlled penetrometer mounted on the tool/penetrometer carriage was used to check for uniformity at three designated locations on the bin. Samples were also taken at the three locations for dry density and moisture content determinations. There were no significant variations in soil properties within the test bed. In order to check for the usefulness of the dynamometer, preliminary investigations were carried out using a simple tillage tool. The tool was a plane narrow blade (5.1 cm wide, 22.9 cm deep). Three sets of experiments were conducted. In the first series, the blade was operated at 45° rake angle, speed of 0.1 m/s and different depths of 3.8, 7.6, 11.4, 15.2, 19.1, 22.9 cm. In the second set, it was operated at 19.1 cm depth, speed of 0.1 m/s and different rake angles of 30, 45, 60, 75, 90°. In the third set, depth (22.9 cm) and rake angle (45°) were constant but speed was variable (0.25, 0.5, 0.75, 1, 1.25, 1.5, 1.75, 2 m/s). Each experiment was repeated three times.

In each case, the desired rake angle was obtained by manual adjustments on the tool holder. The desired depth, maximum distance of travel and maximum speed required were entered through the computer keyboard. As the carriage moved, the measurement and control system acquired force data (F_x , F_z , M_y)

simultaneously and continuously from the extended octagonal ring dynamometer.

4.4 Data Handling and Analysis

The data were observed in real time as the experiments progressed through graphic display which was part of the measurement system. At the end of each of the experiments, the data were stored in both the personal computer (PC) hard disk and floppy disks, for subsequent analysis.

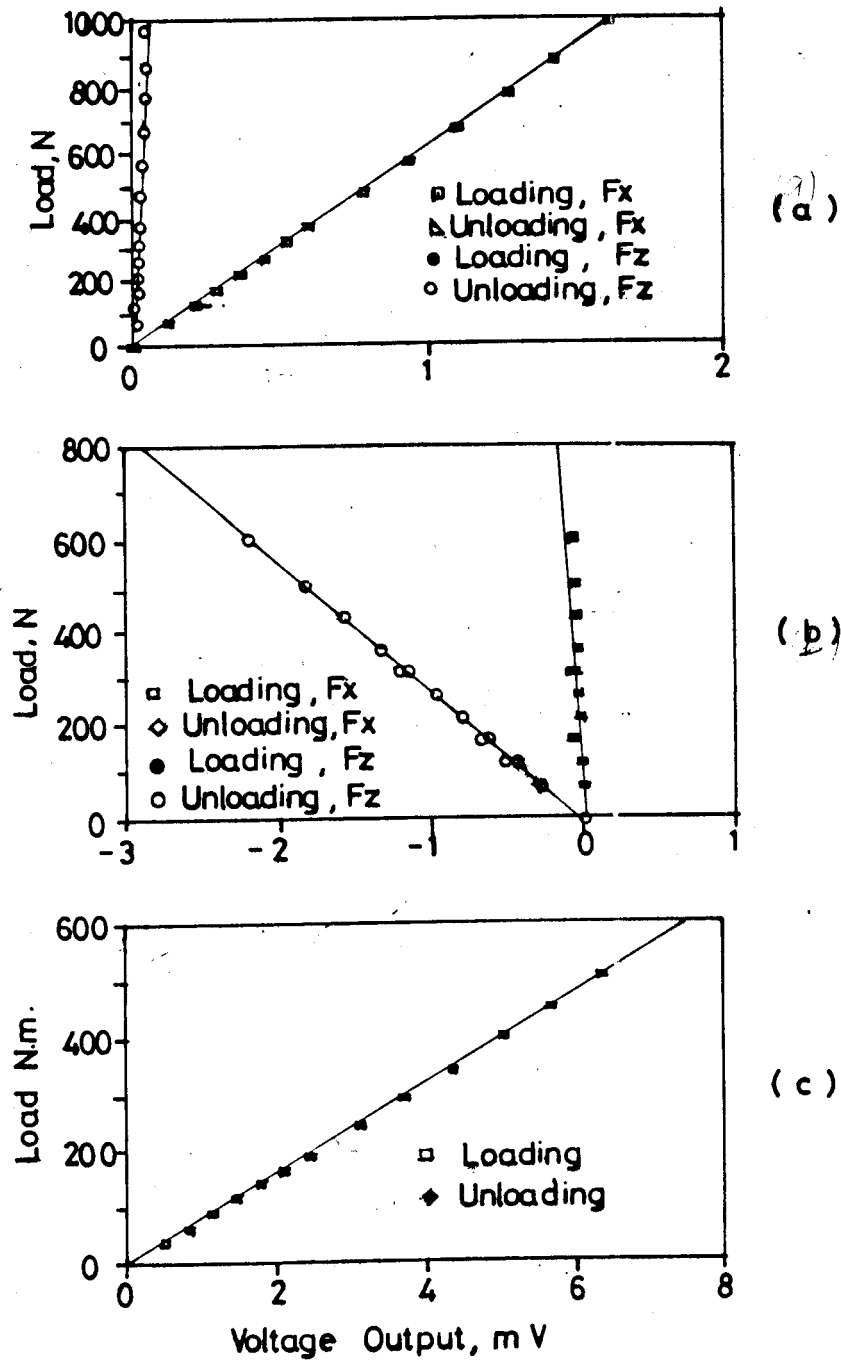
5. PERFORMANCE EVALUATION RESULTS

5.1 Dynamometer Calibration

A sample of the loading and unloading curves for one of the two dynamometers shown in Fig. 10 indicates a linear response within the load range. No hysteresis was noticed in any of the outputs. A linear regression model was fitted to the data in each case:

$$Y = \beta_0 + \beta_1 X \quad (21)$$

Where Y is the relevant load (F_x , N; F_z N; or M_y , N.m); β_0 is the regression constraint, β_1 is the slope of the regression line and X is the voltage output, mV. The values of the β_0 and β_1 obtained for the different loads and dynamometers are shown in Table 3, along with the R^2 values



Calibration curves for one of the dynamometers (a) horizontal force (Fx), (b) vertical for (Fz), (c) moment (My).

Table 3: Regression coefficients for dynamometer calibration

Load	EORD1			EORD2		
	β_0	β_1	R^2	β_0	β_1	R^2
F_x	207	0.8	0.99	603	5.6	0.99
F_z	208	2.6	0.99	-276	-2.2	0.99
M.	22	0.2	1.00	80	-0.4	1.00

F_x = Horizontal force, N; F_z = Vertical force, N; M_y = Moment, N.m; EORD1 - Smaller dynamometer; EORD2 - Bigger dynamometer

5.2 Sensitivity and Rigidity

To obtain the sensitivity of the bridges, the reciprocal of the slope of the regression lines were obtained to give the voltage output per unit load. Since the bridges were powered by a 5 V supply, these values were divided by 5 to obtain the sensitivity in terms of voltage output per unit applied voltage per unit load. The values obtained are presented in Table 4 along with the predicted ones obtained from the design equations presented earlier.

Table 4: Sensitivity of the dynamometers

Parameter	EORD1	EORD2
Predicted sensitivity. F_x ($\mu\text{V}/\text{N.V}$)	0.864	0.622
Measured sensitivity. F_x ($\mu\text{V}/\text{N.V}$)	0.964	0.332
Cross sensitivity. F_x (%)	1.48	0.003
Predicted sensitivity. F_z ($\mu\text{V}/\text{N.V}$)	0.957	0.689
Measured sensitivity. F_z ($\mu\text{V}/\text{N.V}$)	0.963	0.726
Cross sensitivity F_x (%)	2.47	5.08
Predicted sensitivity. M_y ($\mu\text{V}/\text{N.V}$)	6.915	3.486
Measured sensitivity. M_y ($\mu\text{V}/\text{N.V}$)	8.961	2.51

EORD1- Smaller dynamometer. EORD2 - Bigger dynamometer

Cross sensitivity was checked between F_x and F_z .

This was obtained as the variation in the signal output from one channel when loading is in the other direction. When the load was in X direction, there was some variation in F, signal as shown in Fig. 10. Linear regression equations were also fitted to this. Using these, the cross sensitivity was computed and compared to the actual sensitivity to obtain the percent cross-sensitivity presented in Table 4.

A summary of the characteristics of the two dynamometers (Table 4) shows that the experimentally obtained sensitivity agrees with the theoretically predicted ones for the two forces. The cross sensitivity was also within acceptable limits (less than 6%).

5.3 Effect of Tool Parameters on Measured Forces

A typical load-distance history of the tillage tool is shown in Fig. 11(a). The loads initially increased to a maximum at about 500 mm forward travel and stabilized at this value remaining essentially constant for the rest of the run. The initial increase agreed with the exponential (hyperbolic) stress- strain relationship hypothesized for soils in quasi- static failure [26]. The figure shows that the soil forces fluctuated about the mean. The forces

increased to the maximum and dropped sharply to values below the mean and started to increase in a cycle. The three forces were in phase. This sort of response which is attributed to cyclic failure of the soil has been obtained elsewhere [5, 19]. Fig. 11 (b) shows that draught and vertical force increased generally with depth. This type of response is typical of draught and vertical force [10].

Fig. 11(c) shows the effect of rake angle on draught and vertical force. Draught increased with rake angle but vertical force decreased (although this means an increase in the negative direction). The vertical force decreased as rake angle increased, became zero at rake angle of about 65° . The physical interpretation of this change in sign has been given elsewhere [19]. Tool forces generally increased with speed as shown in Fig. 11 (d). This type of response is typical of force- speed relationships [1]. The expected response obtained in these experiments confirmed that the dynamometer and the measurement system were capable of indicating changes in tool forces as a result of changes in operating parameters.

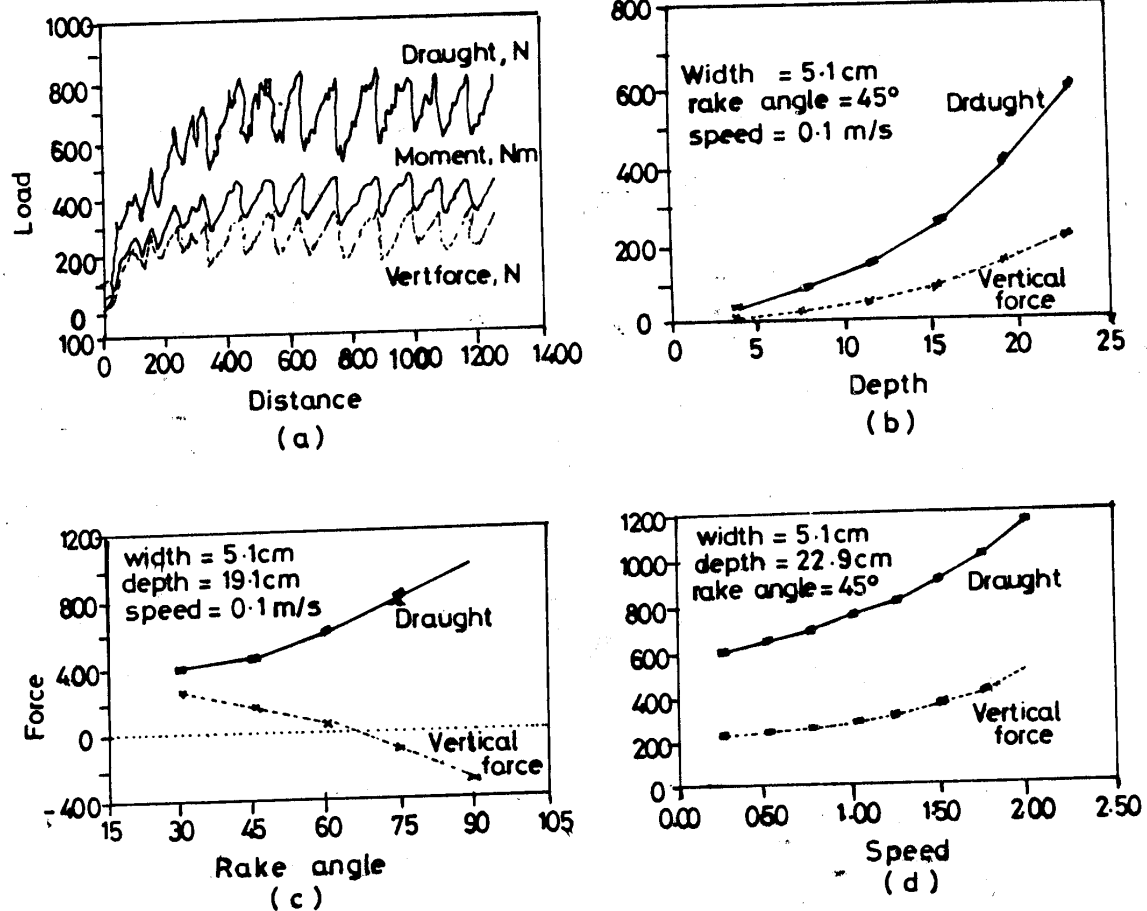


Fig 11: Typical results obtained with dynamometer (a) load distance history (b) effect of depth, (c) effect of rake angle (d) effect of speed on tool forces

6. CONCLUSION

Two extended octagonal ring dynamometers were designed to measure a horizontal force, a vertical force and a moment in the plane of these forces for a plane tillage tool in a soil bin. The design was based on a review of the principles

and experiences reported in the literature. Although the principles are based on that of an extended circular ring, the design equations were found to be adequate for predicting the performance of the transducer.

The transducer output was found to be

linear, no hysteresis effect was observed and maximum cross sensitivity was less than 6%. The dynamometer system was integrated into a computer based measurement and control system for a laboratory soil bin and has provided reliable and useful data on a series of soil-tool interaction investigations.

NOMENCLATURE

b = width of ring, mm
 δ_v = deflection, mm
 E = modulus of elasticity, GPa
 EORD = Extended Octagonal Ring Dynamometer
 ε = strain, mm/mrn
 F = gauge factor of strain gauge
 F_x = horizontal force, N
 F_z = vertical force, N
 F_{xc} = cross sensitivity for F_x
 F_{zc} = cross sensitivity for F_z
 I = moment of inertia, mm
 K = L/R
 K_1 = strain dimensionless group for moment
 K_2 = stiffness dimensionless group for moment
 K_3 = strain dimensionless group for F_x
 K_4 = strain dimensionless group for F_z
 l = length of beam, m
 2L = distance between ring centres, mm
 M_y = moment, Nm
 n = number of active arms of the bridge
 N = safety factor based on yield strength
 M = maximum allowable moment, Nm
 M_φ = moment in the ring due to the forces F_x and F_z , Nm
 α = rotation of the top of the ring due to moment M, deg
 ω_0 = natural frequency of tool bar, Hz
 R = mean radius of ring, mm
 σ_w = design stress, MPa
 σ_y = yield stress, MPa
 t = thickness of ring, mm
 V = voltage, mV
 V_0 = wheatstone bridge output (V)
 V_i = wheatstone bridge excitation (applied) voltage (V)

φ = angular position on the ring

ACKNOWLEDGEMENTS

This work is part of a Ph.D dissertation supervised by Dr. K.C. Watts at the Technical University of Nova Scotia (TUNS), Halifax, Canada. Sponsorship was by the CIDA-UNN-TUNS Linkage Project. Dr. R.L. Schafer of the United States National Soil Dynamics Laboratory, Arburn, USA offered useful advice. Fabrication and wiring of the dynamometers were by the technical staff of TUNS.

REFERENCES

1. Stafford, J.V. A versatile high speed soil tank for studying soil and implement interaction. *J. Agric. Engr. Res.* 24: 57 - 66, 1979.
2. Perumpral, J.V., L.C. Chance, F.E. Woeste and C.S. Desai. A matrix method for force and moment analysis on a tillage tool. *Trans. Am. Soc. Agric. Engrs.* 23(5): 1 072 - 1075, 1980.
3. Reid, J.T., L.M. Carter and R.L. Clark. Draft measurements with three-point hitch dynamometers. *Trans. Am. Soc. Agric. Engr.* 28(1): 89 - 93, 1985.
4. Bowers, C.G. Jr. Tillage draft and energy measurements for twelve South Eastern soil series. *Trans. Am. Soc. Agric. Engrs.* 32(5): 1492 - 1502, 1989.
5. Salokhe, V.M., S. Manzoor and D. Gee- Clough. Pull and lift forces acting on single cage wheel lugs. *Am. Soc. Agric. Engr. (ASAE) Paper No.* 89 - 1049, ASAE St. Joseph, MI 49085-9659, 1989.
6. Godwin, R.J. An extended octagonal ring transducer for use in tillage studies. *J. Agric. Engr. Res.* 20: 347 - 352, 1975.
7. Cook, N.H., and E.R. Rabinowicz. *Physical measurement and analysis.*

- Addison- Wesley Pub, Co. Inc. NY pp. 160 - 165, 1963.
8. Ayers, P.D., K.V. Varma and M.N. Karrim. Design and analysis of electro- hydraulic draft control system. *Trans. Am. Soc. Agric. Engrs.* 32(6): 1853 - 1855, 1989.
 9. Leonard, J J. An extended octagon rigid draw bar dynamometer. *Agric. Engr.* Australia. 9(1): 3 - 8,1980.
 10. Owen, G.T. H. Drummond, L. Cobb and R.J. Godwin. An instrumentation system for deep tillage research. *Trans. Am. Soc. Agric. Engrs.* 30 (6): 1578 - 1582, 1987.
 11. O'Dogherty, MJ. A dynamometer to measure the forces on a sugar beet topping knife. *J. Agric. Engr. Res.* 20: 339 - 345, 1975.
 12. Riley, T.W., and J.M. Fielke. Use of a two force dynamometer for direct drilling point evaluation. Conference on Agricultural Engineering, Hawkesbury Agricultural College, NSW, Australia, 1988.
 13. Thaku, T.C. and R. J. Gowin. Design of extended octagonal ring dynamometer rotary tillage studies. *Agric. Mech. in Asia, Africa and Latin America*, 19(3): 2) - 28, 1988.
 14. Loewen, E.G., E.R. Marshall and M.C. Shaw. Electric strain gauge tool dynamometers. *Proc. Soc. for Exp. Stress Analysis*, 8(2): 1 - 16, 1951
 15. Cook, N.H., E.G. Loewen and M.C. Shaw. Machine tool dynamometers: a current appraisal. *American Machinist*. May 10, 1954.
 16. Loewen, E.G. and N.H. Cook. Metal cutting measurements and their interpretation. *Proc. Soc. for Exp. Stress Analysis*, 13(2): 57 - 62, 1956.
 17. Hoag, D.L. and R.R. Yoerger. Analysis and design of load rings. *Trans. Am. Soc. Agric. Engrs.* 18(5): 995 - 1000, 1975.
 18. Girma, G. Multi component dynamometer for measurement of forces on plough bodies. *J. Agric. Engr. Res.* 42: 85-96, 1989.
 19. Siemens, J.C., J.A. Weber and T.H. Thornburn. Mechanics of soil as influenced by model tillage tools. *Trans. ASAE* 8(1): 1 - 7, 1965.
 20. Dally, J.W. and W.F. Riley. *Experimental stress analysis*. 2nd Edition. McGraw- Hill Book Co., NY, pp. 217 - 261,1978.
 21. Kocher, M.F. and J.D. Summers. Design of drawbar transducers for measuring dynamic forces. *Trans. ASAE* 30(1): 70- 74, 1987.
 22. Summers, J.D., M.F. Kocher and J.B. Solie. Frequency analysis of tillage tool forces. *International Conference on Soil Dynamics Proc. 2: 377 - 383, 1985.*
 23. Onwualu, A.P. and K.C. Watts. A control system for a hydraulically powered soil bin. ASAE Paper No.89 - 1570. *Presented at the 1989 international Winter Meeting of the ASAE, New Orleans, Louisiana, 1989.*
 24. Onwualu, A.P. and K.C. Watts. Development of a soil bin test facility., ASAE Paper No. 89 - 1106. Presented at the 1989 *International Summer Meeting jointly sponsored by the ASAE and CSAE, Quebec Municipal Convention Centre, Quebec, Canada, 1989.*
 25. Onwualu, A.P. *Tool factors affecting sandy soil interaction with plane blades in a soil bin*. Unpublished Ph.D thesis, Technical University of Nova Scotia, Halifax, Canada, 1991.
 26. Duncan, J.M. and c.Y. Chang. Non-linear analysis of stress and strain in soil. *J. Soil Mechanics and Foundations Div., ASCE* 96(SM5):1629-1653, 1970.